



1 **Assessment of rockfall hazard on the steep-high slopes:**

2 **Ermenek (Karaman, Turkey)**

3

4 **Hidayet Tağa and Kıvanç Zorlu**

5

6 Mersin University, Department of Geological Engineering, Mersin, Turkey

7

8 **Abstract**

9

10 Ermenek is one of the curious settlement areas because of its topographical features in
11 Karaman (Turkey). The city is located in northern side of the very steep cliffs formed by
12 jointed limestone which are suddenly increased from 1250 m to 1850 m. Moreover, these
13 cliffs having almost 90° slope dip are the main rockfall source areas due to their lithological
14 characteristics, climatic effects and engineering properties of rock units. Up to now,
15 depending on rockfall events, almost 500 residences were damaged severely, and losses of
16 lives were also recorded in Ermenek. The rockfall phenomenon are initiated by discontinuities,
17 lithological changes, weathering and freeze-thaw process in the study area. In this study,
18 extensive fieldwork including determination of location and dimension of hanging, detached
19 and already fallen blocks, a detailed discontinuity survey, description of geological,
20 morphological and topographical characteristics was performed. Besides, rockfall hazard is
21 evaluated by two-dimensional rockfall analyses along 10 profiles. During the rockfall
22 analyses; run out distance, bounce height, kinetic energy and velocity of various size of
23 blocks for each profiles are determined by using RocFall v4.0 software. The results obtained
24 from rockfall analyses were used to map the areas possible rockfall hazard zones and
25 rockfall source areas were interpreted.

26

27 According to rockfall analysis, field study and laboratory testing, protective and preventive
28 recommendations can be suggested for the areas under rockfall threat. But, the most widely-
29 known remedial measures in literature such as trenches, retaining walls (barrier), wire
30 meshes, cable/stretching nets and rock bolting etc. are not sufficient in the study area, due to
31 topographical, atmospheric and lithological features. For these reasons, firstly total
32 evacuation of the danger zone should be applied and then hanging blocks in the reachable
33 locations can be removed taking safety measures in this area to make it safer for the living
34 people.

35

36 **Keywords:** Hazard, Rockfall, Limestone, Zonation map, Ermenek.

37



38 Introduction

39

40 Rockfall is a fast movement of the blocks which are detached from the bedrock along
41 discontinuities that slides, rolls or falls along vertically travels down slope by bouncing and
42 flying along trajectories (Varnes, 1978; Whalley 1984; Dorren 2003). Due to their high speed
43 and energy, rockfalls can be admissible as a substantially destructive mass movement
44 resulting in significant damage and loss of live. This movement is mainly controlled by the
45 geological conditions of the rock units, climatic influences and the weathering processes.
46 Besides, discontinuity patterns and the related intersections are also played an important role
47 of the size and shape of the detached blocks (Perret et al. 2004).

48

49 The slope characteristics are very significant factors for the rockfall events. The normal (r_n)
50 and tangential (r_t) components of coefficient of restitution, are related to the slope
51 characteristics that control behavior of the falling blocks and they are the most crucial input
52 parameters for rockfall analyses (Chau et al. 1996). Both components of coefficient of
53 restitution are related to material covering the surface, vegetation, surface roughness, and
54 radius of the falling rocks (Dorren et al., 2004). The coefficient of restitution with normal and
55 tangential components are best determined by the field tests and back analysis of the fallen
56 blocks. Although many researchers are revealed several techniques to determine the
57 coefficient of restitutions, these parameters should be identified individually for each side
58 because of the different geometrical features and mechanical properties of the slopes
59 (Agliardi and Crosta 2003; Dorren et. al, 2004; Evans and Hungr 1993; Robotham et al.
60 1995; Pfeiffer and Bowen 1989; Ulusay et al. 2006; Topal et al 2007; Topal et al., 2012, Buzzi
61 et al 2012). On the other hand, slope inclination and slope properties are also affecting the
62 runout distances of the falling blocks (Okura et al., 2000). The slope surface of a hard rock
63 and free from vegetation cover is more dangerous then the surface covered by vegetation or
64 talus material because of the fact that it does not retard the movement of falling blocks.

65

66 To simulate fall of a blocks down a slope and to compute rockfall trajectories, various two
67 dimensional (2D) or tree dimensional (3D) and 2D-3D Discontinuous Deformation Analysis
68 (DDA) programs have been developed and tested during the last few years and many of
69 study considering with rockfall analyses and simulations are carried out. Additionally, the
70 rockfall susceptibility and hazard maps are produced using both two and tree dimensional
71 rockfall analysis technique considering with mostly traveling distance of falling blocks.
72 (Bassato et al. 1985; Falcetta 1985; Bozzolo and Pamini 1986; Hoek 1987; Pfeiffer and
73 Bowen 1989; Azzoni et al. 1995; Jones et al. 2000; Guzetti et al. 2002, Guzetti et al, 2003;
74 Agliardi and Crosta 2003; Schweigl et al 2003; Perret et al 2004; Yilmaz et al. 2008,



75 Tunusluoglu and Zorlu 2009, Binal and Ercanoglu 2010; Zorlu et. al 2011; Katz et al 2011;
76 Topal et al 2012; Chen et al. 1994; Keskin 2013).

77

78 In this study, rockfall analyses are performed in Ermenek district located on very steep cliffs
79 considering past recorded phenomenon and recently ongoing threats of event (Fig 1). The
80 rockfalls occur very close to residential area and already damaged the houses and
81 unfortunately have been losses of lives. To reveal the rockfall potential of the study area, an
82 extensive field work including detailed discontinuity survey, determination of location and
83 dimensions of hanging, detached and already falling blocks, and also back analyses was
84 carried out. Two dimensional rockfall analyses are conducted along 10 selected profile to
85 assess the block trajectories, runout distance, kinetic energy and bounce high of the blocks,
86 based on field and laboratory test data. Then a rockfall danger zonation map was produced
87 by means of the results obtained from rockfall analyses and areal extension of rockfall was
88 delineated. When considering location, climatic adversities and geological factors of the study
89 area, some remedial measures can be arguable. Despite the unfavourable conditions,
90 possible remedial measures are suggested for the study area.

91

92 **Geological Settings**

93

94 The Ermenek basin is one of the Neogene intramontane molasse basin formed in Central
95 Taurides, the orogenic belt's segment stretching between the Isparta angle to west and the
96 Ececi Fault to the east (Özgül, 1976; Ilgar and Nemec, 2005). The Ermenek basin and the
97 adjacent Mut Basin lies between the Cukurova basin complex to the east and the Antalya
98 basin complex to the west and is situated within the central part of the Taurides, an E-W
99 trending orogenic belt that originated through compressive deformation during the initial
100 stage of closure of the southern branch of the Neo-Tethyan ocean in the Early Cenozoic
101 (Safak et al. 1997). The basins evolved as extensional grabens related to preexisting
102 fractures. Deposition resumed in Early Miocene time, with Mut basin hosting alluvial
103 sedimentation and the Ermenek basin becoming a large clastic lake. The two basins, formed
104 as separate intermontane depressions, were then inundated by the sea near the end of the
105 Early Miocene and jointly covered with an extensive, thick succession of late Burdigalian-
106 Serravalian carbonates, including reefal and platform limestones (Ilgar and Nemec, 2005).

107

108 The tectonic history of Southern Turkey can be summarised into three major periods; (1) Late
109 Palaeozoic to Middle Eocene: formation of the Tethyan orogenic collage. (2) Middle Eocene
110 to Middle Miocene: Tauride Orogeny during continued north-south convergence and collision;
111 migration of deformation front south of Turkey. (3) Late Miocene to recent: collision of



112 Eurasia with the Arabic Plate and start of the Neotectonic Regime (Basnt et al 2005). Due to
113 this complex tectonic movement the Taurus Belt exhibits very complicate stratigraphic
114 sequence and litological diversity (Fig 2).

115

116 The basement of the Ermenek basin consists of Paleozoic and Mesozoic units, which are
117 generally exposed at the southern part of the basin. Palaeozoic units compise of shale,
118 limestone, dolomitic limestone, and quartzite. While Lower-Middle Triassic units contains
119 limestone, shale; Upper Triassic units consists of sandstone, conglomerate and limestone;
120 Jura-Cretaceous time is represented by dolomitic limestone (Gul and Eren, 2003). Eocene
121 and Palaeocene sedimentary units contain fossiliferous limestone (Tepebasi Formation)
122 unconformably overlie the Cretaceous limestone and ophiolitic melange. Oligocene lacustrine
123 deposits represent by Pamuklu Formation including coal layer as Yenimalle Formation,
124 overlies unconformably Eocene-Oligocene units in the area. The Yenimahalle Formation has
125 a great lateral extentention in the Ermenek basin consists of six main facies association,
126 which range from alluvial to offshore lacustrine deposits, up to 300 m in thickness. Middle
127 and Upper Miocene units unconformably overlie the Lower Miocene unit in the basin are
128 characterized by Mut, Köselerli and Tekecati Formations. Koselerli Formation comprises
129 claystone, limestone, clayey limestone, gravelly sandstone and marl deposits representing
130 centre of the reef (reef core facies). Mut formation also consist of reef limestones deposits in
131 shallow marine environment including limestone with clayey or fossiliferous, and distinctive
132 patch reefs are common in this formation (Gul and Eren, 2003). The last unit of the Miocene
133 age sequence of the basin is Tekecati Formation consists of limestone, fossiliferous
134 limestone, clayey limestone and mudstone as assessed typically shallow sea sediment
135 belong to a reefal environment (Yurtsever et al. 2005). All these formations of Middle and
136 Upper Miocene also interfinger and they have transitional contacts with each other (Fig 3).

137

138 A Digital Elevation Model (DEM) of the study area was constructed by implementation of
139 contour lines of 1:25,000 scale topographic maps with an equidistance of 10 m. When
140 considering DEM, the altitude values of the northern and the south-eastern parts of the study
141 area vary from 1,200 to 1,860 m (Fig 4a), slope gradients exceed 90° from 0° (Fig 4b) and
142 the general physiographic trend of the study area is about S-SE (Fig 4c)

143

144 **Field investigation and engineering properties of the rock**

145

146 Rockfall events are observed in the very steep cliffs formed by jointed limestone which are
147 suddenly increased from 1250 m to 1850 m. The limestone of Mut Formation is not form from
148 a single lithological property it is also formed by succession of different lithologies which is



149 one of the triggering factor of the rock fall events. Owing to its complex lithological structure,
150 the field studies are also carried out more detailed considering with lithological differences. A
151 systematic sampling was conducted to determine the lithological and geomechanical
152 properties of Mut formation with different facieses. Petrographic investigations of the
153 limestone specimens from the systematic sampling along X-X' line (Fig 5) of formation
154 consists of routine observations under polarized microscope. According to the results of the
155 petrographic analyses, the specimens are formed by four lithological units such as,
156 fossiliferous limestone, claystone-marl, clayey limestone and limestone. The results of
157 petrographic thin-section analyses are summarized in Table 1.

158

159 The X-ray diffraction analyses (XRD) are also applied to the specimens to assess the relative
160 quantity of minerals (Table 1). The XRD diffractograms are obtained at General Directorate of
161 Mineral Research and Exploration X-Ray Laboratory. The X-ray diffraction and the thin-
162 section analyses results show it is obvious that Mut formation arise four different litological
163 units.

164

165 During the field studies a series of systematic scan-line surveys were carried out to
166 determine the orientation and spacing of discontinuities based on ISRM (1978) and ISRM
167 (1981). According to scan-line survey, five main discontinuity sets were determined via
168 contour diagrams using a computer program, name of DIPS 5.1 (RocScience Inc. 2006). The
169 dip and dip direction of values of the major sets are 86/154, 85/210, 87/173, 84/077 and
170 55/155 (Fig 6). The discontinuities have high persistence (20 m), very tight to very open
171 aperture (from 0.1 mm to 10 cm) without infilling. The discontinuity surfaces are rough,
172 undulating and groundwater seepage is not existed through discontinuities surface. The
173 average spacing value of discontinuities is determined as 170 cm. and the discontinuity
174 spacing histogram is given in Fig 7.

175

176 Kinematic analyses of the discontinuities are conducted for western, northern and eastern
177 slopes of the study area. Kinematic analyses show that two different failure types observed
178 on the slopes. Although sliding is encountered as a main failure type on the each slope,
179 toppling type of failure is occurred only western and northern part (Fig 8).

180 During the field work, already fallen and hanging blocks in various dimensions were observed
181 in the study area. For real approaches at rockfall modeling, size, location and runout distance
182 of fallen blocks were determined (Fig 9). In addition to various sizes of hanging blocks,
183 different rockfall source area was also observed during the field study (Fig 10). Besides,
184 block samples were taken in the field for laboratory test. While taken block sample,
185 systematic sampling was carried out from bottom to top of slopes due to its different



186 lithological and mineralogical features of Mut formation. The tests performed in the laboratory
187 are unit weight, apparent porosity, void ratio, water absorption by weight, water absorption by
188 volume and uniaxial compression strength for each sampling zone. When applying the tests,
189 the procedures suggested by ISRM (1981) suggested methods are taken into consideration.
190 The average unit weight of limestone samples (23.9 kN/m^3) were the highest than the
191 fossiliferous limestone (22.2 kN/m^3), claystone-marl (20.4 kN/m^3), and clayey limestone (21.5
192 kN/m^3) sample. The uniaxial compressive stress values of samples were found vary in a
193 large range. The average uniaxial compressive strength values of limestone, fossiliferous
194 limestone and clayey limestone were 55 MPa, 48 MPa and 36 MPa respectively. The
195 standard core sample can not be extracted from highly weathered zones of claystone-marl
196 for uniaxial compression tests. To cope with this difficulty, the Schmidt hammer index test
197 was performed in the field. The average Schmidt hammer rebound number of the claystone-
198 marl was obtained as 33 and the uniaxial compression strength value was found as 22 MPa
199 indirectly. The results obtained from the tests with statistical evaluations are given in Table 2.

200

201 **Rockfall analyses**

202

203 Various two or three-dimensional computer program are existed to simulate fall of boulder
204 and compute rockfall trajectories, (Bassato et al. 1985; Falcetta 1985; Bozzolo and Pamini
205 1986; Hoek 1987; Pfeiffer and Bowen 1989; Azzoni and de Freitas 1995; Jones et al. 2000;
206 Guzzetti et al. 2002). In this study, rockfall simulations of Ermenek steep cliffs carried out
207 using Rockfall V.4 software (Rockscience Inc. 2002). Rockfall V.4 is a two-dimensional
208 software program performing statistical analyses of rockfall and calculation engine behaves
209 as if the mass of each rock is concentrated in an extremely small circle. While simulate
210 rockfall trajectories, any size or shape effects must be accounted for by an approximation of,
211 or adjustments to, other properties (Rockscience Inc. 2002). Some crucial parameters are
212 required to design block trajectories and rockfall analysis, the coefficient of restitution (normal
213 and tangential), slope geometry, roughness of slope and weight of hanging blocks. The slope
214 geometry is revealed from 1/1.000 scale topographic map. When considering lithological
215 features, distance from settlement district and location of rockfall source areas, ten slope
216 profile selected for rockfall simulation analysis (Fig 11). In the field study, hanging blocks are
217 determined and weight of reachable block is calculated by using unit weight and volume of
218 the rock (Fig 12). The hanging or detached blocks had various dimensions due to the
219 discontinuity orientation, spacing and their mineralogical composition affected by weathering
220 processes. The calculated hanging blocks weights vary between 75 kg and 9.800 kg for
221 different rockfall source areas (see Fig 10). For selected ten profiles, different rock masses
222 (100 kg, 1.000 kg and 10.000 kg) were used in the rockfall analyses considering block sizes



223 which are ideally represented field conditions. Initial velocity of blocks was preferred 0 m/s in
224 the analyses considering the situation of the each block.

225

226 The slope characteristics are very important factors for the rockfall event because of the fact
227 that the slope properties control the behavior of the falling blocks as runout distance of the
228 blocks (Okura et al. 2000). The slope surfaces was played a considerable role in movement
229 of falling or rolling blocks moving through the slopes. The slope faces are free from
230 vegetation cover, they do not retard the movement of blocks. In this case, the blocks can be
231 reached farther distance, on the contrary of the surface covered by vegetation or talus
232 material. Because, the vegetation or talus material absorbs a high amount of the energy of
233 the falling rock and will probably stop it (Hoek 2007). The retarding capacity of the slope
234 surface material is expressed mathematically normal (R_n) and tangential (R_t) coefficient of
235 restitution are affected by the composition of the material covering the surface and slope
236 roughness. The coefficient of restitutions can be obtained from back analyses in the field or
237 theoretical estimations (Agliardi and Crosta 2003; Dorren et. al, 2004; Evans and Hungr
238 1993; Robotham et al. 1995; Pfeiffer and Bowen 1989; Ulusay et al. 2006; Topal et al. 2007).
239 Back analyses were performed to determine the coefficient of restitution with ten blocks in the
240 field considering the size and the shape of the blocks and the slope characteristics (Fig 13).
241 The results of the analyses, normal and tangential coefficients of restitution values belong the
242 fallen rocks are determined as (0.33 ± 0.04) and 0.63 ± 0.19 respectively. In addition to
243 coefficients of restitution, friction angle was determined by field back analyses as 32.5° .
244 During the rockfall analyses 1.000 rock blocks were thrown. The slope roughness which is
245 another input parameter of rockfall simulation analyses was taken as 2° in based on the
246 angle between rough surfaces. The input parameters used for rockfall analyses are given in
247 Table 3.

248

249 Rockfall simulation analyses were performed ten profiles as mentioned above. The limestone
250 and fossiliferous limestone units resisting against weathering, upper zones of weaker
251 lithological unit claystone-marl accepted as rockfall source areas, based on field conditions
252 (Fig 14). During the rockfall analyses, different rock masses (100 kg, 1.000 kg, 10.000 kg)
253 were used for each profiles considering the real masses of hanging blocks in the study area.
254 One of the typical examples of a rockfall trajectory is given in Fig. 15 .The runout distance,
255 bounce height, kinetic energy and velocity of the blocks were predicted by rockfall analyses.
256 According to the results of the analyses, maximum runout distance reaches 660 m, kinetic
257 energy 1.750.000 kJ and velocity is 46.3 m/s for the free falling of the 1000 kg blocks. The
258 results of analyses are summarized in Table 4. A rockfall danger zone map was produced by
259 using the results obtained from rockfall analyses considering maximum runout distance of



260 falling blocks Fig 16. According to map, areal extension of all blocks for each profile would be
261 able to reach to the roads or settlement area. It is apparent that the settlement area was
262 located in the danger zone. Although some preventative measures can be applied to reduce
263 rockfall hazard, it was directly depend on topographical and lithological factors of the
264 potential rockfall source area. Also the aesthetic and socio-economic conditions were limited
265 to the existing preventative measurements. Construction of trenches, retaining walls (barrier),
266 wire meshes, cable/stretching nets, rock bolting and evacuation of the danger zone can be
267 used as preventive measures in the rockfall areas. But, the most widely-known remedial
268 measures in literature are not proper in the study area, due to topographical and lithological
269 features. Thus, to apply trenching and fencing is not possible due to the big size of hanging
270 blocks have relatively high kinetic energy and bounce height. Rock bolting can not be applied
271 higher elevations because the slopes have considerably steep cliffs and large block sizes.
272 Therefore, it is recommended that the hanging blocks in the reachable locations should
273 removed taking safety measures. Although total evacuation of the danger zone is not
274 preferred by the residents, in opinion of the authors of this study, it is indispensable in the
275 study area.

276

277

278 **Results and conclusions**

279

280 Ermenek is a spectacular settlement area located in very steep cliffs with a height of 1850 m.
281 The settlement was subjected to rockfall event several times and resulted in loss of life and
282 property. During the fieldwork and depending on laboratory test results, the rockfalls were
283 initiated by discontinuities, weathering process and characteristics of limestone having
284 different lithological facieses. Considering the scan-line survey, five main discontinuity sets
285 were determined. To understand of rockfall mechanism, relevant with lithological features, X-
286 ray diffraction and thin-section analyses were taken into consideration and revealed that the
287 limestone formation are formed by four lithological units such as, fossiliferous limestone,
288 claystone-marl, clayey limestone and limestone. Thus rockfall occurs uppermost level of
289 limestone and fossiliferous limestone due to existence of weaker claystone-marl at the lower
290 level of the facies.

291

292 Two dimensional rockfall analyses were performed using the data collected from field study
293 and laboratory test results along 10 profiles. Rockfall analyses were indicated that the roads
294 and the settlement area were remaining in the rockfall danger zone. Considering
295 topographical and lithological limitations, commonly used remedial measures are not



296 preferred in present study. Total evacuation and cleaning the loose blocks in accessible
297 locations are recommended.

298

299 **Acknowledgment**

300

301 This research is supported by The Scientific and Technological Research of Turkey,
302 TUBITAK (Project No:107Y071).

303

304 **References**

305

- 306 Agliardi F, Crosta GB: High resolution three-dimensional numerical modelling of rockfalls. *Int*
307 *J Rock Mech Min Sci* 40, 455–471, 2003.
- 308 Azzoni A, de Freitas MH: Experimentally gained parameters, decisive for rockfall analysis.
309 *Rock Mech Rock Eng* 28, 111–124, 1995.
- 310 Bassant, P., van Buchem, F.S.P., Strasser, A. and Gfrqr, N: The stratigraphic architecture
311 and evolution of the Burdigalian carbonate–siliciclastic sedimentary systems of the Mut
312 basin, Turkey. *Sedimentary Geology* 173, 121–150, 2005.
- 313 Bassato G, Cocco S, Silvano S: Programma di simulazione per lo scoscendimento di blocchi
314 rocciosi. *Dendronatura* 6, 34–36, 1985.
- 315 Bozzolo D, Pamini R: Modello matematico per lo studio della caduta dei massi. Laboratorio di
316 Fisica Terrestre ICTS. Dipartimento Pubblica Educazione, Lugano-Trevano, 1986.
- 317 Binal A, Ercanog̃lu M: Assessment of rockfall potential in the Kula (Manisa, Turkey) Geopark
318 Region. *Environ Earth Sci* 61, 1361–1373, 2010.
- 319 Buzzi O, Giacomini A, Spadari M: Laboratory investigation on high values of restitution
320 coefficient *Rock Mech Rock Eng* 45, 35–43, 2012.
- 321 Chau KT, Wong RHC, Lee CF: Rockfall problems in Hong Kong and some new experimental
322 results for coefficient of restitution. *Int J Rock Mech Min Sci* 35, 662–663, 1996.
- 323 Chen H, Chen RH, Huang T: An application of an analytical model to a slope subject to
324 rockfalls *Bull As Eng Geol* 31, 447–458, 1994.
- 325 Dorren LKA A review of rockfall mechanics and modeling approaches. *Prog Phys Geogr* 27,
326 69–87, 2003.
- 327 Dorren LKA, Maier B, Putters US, Seijmonsbergen AC: Combining field and modelling
328 techniques to assess rockfall dynamics on a protection forest hillslope in the European
329 Alps. *Geomorphology* 57, 151–167, 2004.
- 330 Evans SG, Hungr O: The assessment of rockfall hazard at the base of talus slopes. *Can*
331 *Geotech J* 30, 620–636, 1993.
- 332 Falcetta JL: Un nouveau mod"ele de calcul de trajectoires de blocs rocheux. *Revue*
333 *Francaise de Geotechnique* 30, 11–17, 1985.
- 334 Guzzetti F, Crosta G, Detti R, Agliardi F: STONE: a computer program for the three-
335 dimensional simulation of rockfalls. *Comput Geosci* 28, 1079–1093, 2002.
- 336 Guzzetti F, Reichenbach P, Wieczorek GF: Rockfall hazard and risk assessment in the
337 Yosemite Valley, California, USA. *Nat Hazards Earth Syst Sci* 3, 491–503, 2003.
- 338 Gul M and Eren M: The sedimentary characteristics of Dagpazarı patch reef (Middle Miocene,
339 Mut-Icel/Turkey) Carbonates and Evaporites 18, 51–62, 2003.
- 340 Hoek E: Rockfall—a program in BASIC for the analysis of rockfall from slopes. Unpublished
341 note, Golder Associates/ University of Toronto, Canada, 1987.
- 342 Hoek E: Practical rock engineering. Course note, 2007.
- 343 Ilgar, A. and Nemeč, W: Early Miocene lacustrine deposits and sequence stratigraphy of the
344 Ermenek Basin, Central Taurides, Turkey. *Sedimentary Geology*, 173, 233–275, 2005.



- 345 Jones CL, Higgins JD, Andrew RD: Colorado rockfall simulation program version 4.0.
346 Colorado Department of Transportation, Colorado Geological Survey, 2000.
- 347 Katz O, Reichenbach P, Guzzetti F: Rock fall hazard along the railway corridor to Jerusalem,
348 Israel in the Soreq and Refaim valleys. *Nat Hazards* 56, 649–665, 2011
- 349 Keskin I: Evaluation of rock falls in an urban area: the case of Bo azici (Erzincan/Turkey)
350 *Environ Earth Sci* 70, 1619–1628, 2013.
- 351 Okura Y, Kitahara H, Sammori T, Kawanami A: The effects of rockfall volume on runout
352 distance. *Eng Geol* 58, 109–124, 2000.
- 353 Özgül, N: Torosların bazı temel jeoloji özellikleri. *Türkiye Jeol. Kur. Bül.*, 19, 65-78, 1976.
- 354 Perret S, Dolf F, Kienholz H: Rockfalls into forest: analysis and simulation of rockfall
355 trajectories-consideration with respect to mountainous forest in switzerland. *Landslides*
356 1, 123–130, 2004.
- 357 Pfeiffer TJ, Bowen TD: Computer simulation of rockfalls. *Bull Assoc Eng Geol* 1, 135– 146,
358 1989.
- 359 Robotham ME, Wang H, Walton G: Assessment of risk from rockfall from active and
360 abandoned quarry slopes. *Trans Inst Min Metall* 104, A25–A33, 1995.
- 361 Rocscience: RocFall software—for risk analysis of falling rocks on steep slopes. Rocscience
362 user's guide, p 59, 2002.
- 363 Schweigl J, Ferretti C, Noßsing L: Geotechnical characterization and rockfall simulation of
364 slope: a practical case study from South Tyrol (Italy). *Eng Geol* 67, 281–296, 2003.
- 365 afak, Ü: Karaman yöresi Üst Miyosen-Pliyosen istifinin ostrakoda faunası ve ortamsal
366 yorumu. *MTA Dergisi*, 119, 89-102, 1997.
- 367 Topal T, Akin M, Ozden AU: Assessment of rock fall hazard around Afyon Castle, Turkey.
368 *Environ Geol* 53, 177–189, 2007.
- 369 Topal T, Akin M. K., Akin M: Rockfall hazard analysis for an historical Castle in Kastamonu
370 (Turkey), *Natural Hazards* 62, 255-274, 2012.
- 371 Tunusluoğlu MC, Zorlu K: Rockfall hazard assessment in a cultural and natural heritage
372 (Ortahisar Castle, Cappadocia, Turkey). *Environ Geol* 56, 963–972, 2009.
- 373 Ulusay R, Gokceoglu C, Topal T, Sonmez H, Tuncay E, Erguler ZA, Kasmer O: Assessment
374 of environmental and engineering geological problems for the possible re-use of an
375 abandoned rock-hewn settlement in Urgup (Cappadocia) Turkey. *Environ Geol* 50, 473–
376 494, 2006.
- 377 Varnes DJ: Slopemovement types and processes. In: Schuster RL, Krizek RJ (ed) *Landslides,*
378 *analysis and control.* Transportation and Road Research Board, National Academy of
379 Science, Washington, DC, pp 11–33, 1978.
- 380 Whalley WB: Rockfalls. In: Brunnsden D, Prior DB (eds) *Slope stability.* Wiley, New York, pp
381 217–256, 1984.
- 382 Yilmaz I, Yildirim M, Keskin I: A method for mapping the spatial distribution of RockFall
383 computer program analyses results using ArcGIS software. *Bull Eng Geol Environ* 67,
384 547–554, 2008.
- 385 Yurtsever, T. , Ilgar, A. ve Gürçay, B: Ermenek (Karaman)-Mut-Gülnar (çel) Arasında Kalan
386 Tersiyer HavzasınınJeolojik Ve Sedimantolojik ncelenmesi. MTA Rapor No:10776
387 (Unpublised), 2005.
- 388 Zorlu K, Tunusluoglu MC, Gorum T, Nefeslioglu HA, Yalcin A, Turer D, Gokceoglu C:
389 Landform effect on rockfall and hazard mapping in Cappadocia (Turkey). *Environ Earth*
390 *Sci* 62, 1685–1693, 2011.

391
392
393
394
395
396
397
398
399

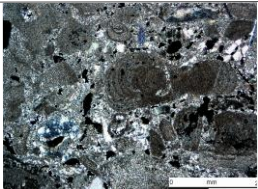
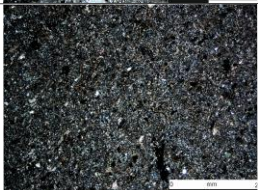
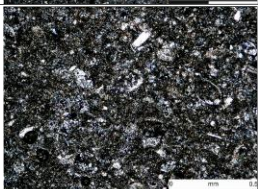
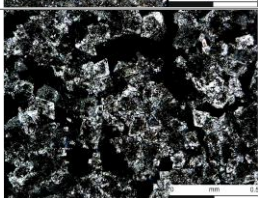


400	
401	
402	
403	List of Tables
404	
405	Table 1 Results of the thin-section petrographic and X-ray analyses
406	Table 2 Laboratory and field test results
407	Table 3 Input parameters used in the rockfall analyses
408	Table 4 Results of the rockfall analyses
409	
410	
411	
412	
413	
414	
415	
416	
417	
418	
419	
420	
421	
422	
423	
424	
425	
426	
427	
428	
429	
430	
431	
432	
433	
434	
435	
436	
437	



438
 439

Table 1 Results of the thin-section petrographic and X-ray analyses

Specimen No	Petrographic description	X-ray analysis result	Microscopic photograph
HK05-1	Limestone	Calcite, Quartz	
HK05-2	Clayey Limestone	Calcite, Quartz Chlorite, Dolomite	
HK05-3	Claystone-Marl	Calcite, Dolomite, Simectite	
HK05-5	Fossiliferous Limestone	Calcite, Dolomite	

440
 441



442
 443
 444
 445
 446

Table 2 Laboratory and field test results

	Limestone				Clayey limestone				Claystone-Marl				Fossiliferous Limestone			
	Max.	Min.	Average	Standart Deviation	Max.	Min.	Average	Standart Deviation	Max.	Min.	Average	Standart Deviation	Max.	Min.	Average	Standart Deviation
Unit weight (kN/m³)	24,3	23,2	23,9	0,31	22,0	21,2	21,5	0,22	20,7	20,2	20,4	0,19	23,6	20,5	22,2	0,99
Void ratio (%)	7,26	3,70	5,33	1,16	19,05	16,62	17,67	0,77	24,37	20,02	21,47	1,28	21,99	7,36	11,88	3,40
Porosity (%)	6,77	3,57	5,05	0,96	16,00	14,25	14,98	0,55	19,59	16,68	17,67	0,86	18,02	6,85	10,47	3,77
Water absorption by weight (%)	2,86	1,45	2,07	0,42	7,39	6,48	6,81	0,29	9,44	7,89	8,48	0,44	8,63	2,86	4,70	1,97
Water absorption by volume (%)	6,77	3,57	5,05	0,96	16,00	14,25	14,98	0,55	19,59	16,68	17,67	0,86	18,02	2,86	10,47	3,77
Uniaxial compressive strength (MPa)	73,4	46,2	55,3	10,58	39,8	32,4	36,1	2,57	27,4	18,1	22,2	3,90	59,6	29,4	48,1	12,08
Schmidt hammer rebound number			55				39				25				48	
Number of Samples			13				11				11				10	

447
 448
 449



450
451
452
453

Table 3 Input parameters used in the rockfall analyses

Parameter	Value
Number of rockfall	1000
Minimun velocity cut off (m/s)	0.1
Coefficient of normal restitution	0.33±0.04
Coefficient of tangential restitution	0.63±0.19
Friction angle()	32.5°
Slope roughness	2
Initial velocity (m/s)	0 ± 0.5

454
455

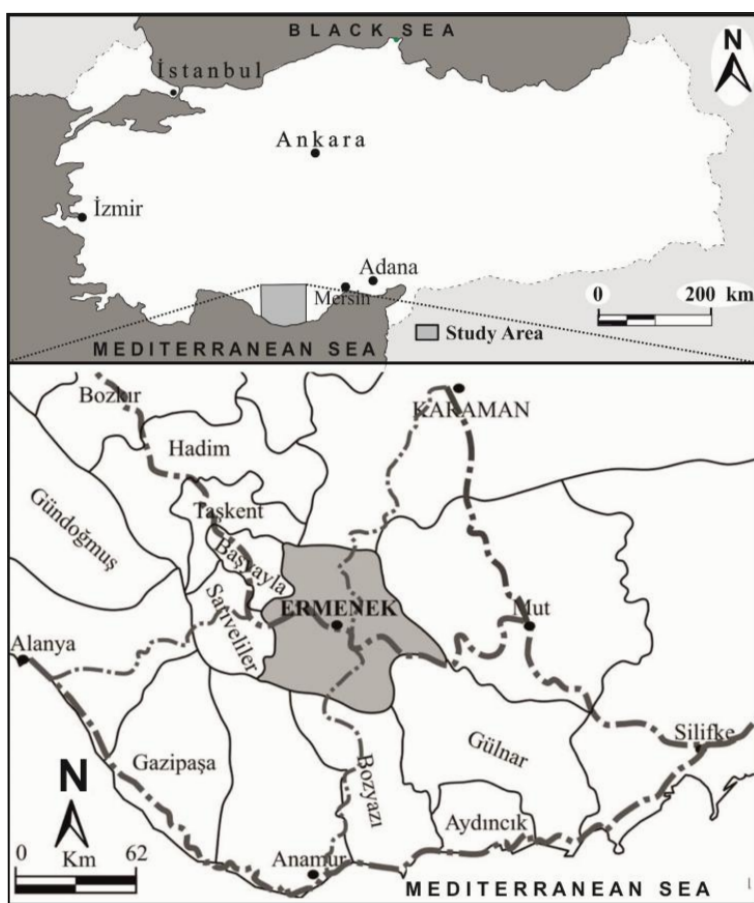


456 **Table 4** Results of the rockfall analyses
 457

Profile Number	Maximum Slope Height (m)	Weight of block (kg)	Runout distance (m)		Bounce height (m)		Kinetic energy(kJ)		Velocity (m/s)	
			Max	Min	Max	Min	Max	Min	Max	Min
1	88	100	683	170	7	0,5	14000	1000	16	1
		1000	585	195	3	0,5	120000	5000	14	2
		10000	480	160	7,25	0,5	1400000	10000	16	2
2	33	100	535	233	2,8	0,5	2200	1025	6,3	2
		1000	280	233	3	0,5	18200	1247	7,21	1,02
		10000	277	222	3,2	0,45	62033	6300	3,27	1,03
3	334	100	272	115	13,25	1,23	14027	60150	16,29	8,23
		1000	275	48	19	2	1750000	7350	46,3	8,23
		10000	263	72	108,5	13,5	11200000	860000	63,5	9,87
4	145	100	323	75	68,3	4,3	34500	6350	28,43	3,45
		1000	312	80	11,8	3,05	583400	54000	34,42	3,02
		10000	325	82	13,8	6,32	6973000	425000	33,25	2,1
5	123	100	273	32	57,32	11,3	64300	8920	36,32	12,32
		1000	281	40	68,32	4,06	670000	33000	33,24	4,2
		10000	283	45	68,3	4,23	6270000	4350000	33,5	6,7
6	103	100	235	12	8	2	102500	5000	46	3,8
		1000	232	11	6,4	1,8	958000	5800	45	4,2
		10000	88	43	18	3,2	10500000	560000	43,5	3,8
7	336	100	7,8	2,8	1,2	0,2	8320	1823	12	5
		1000	7,5	1	1,1	0,18	83000	31000	11,5	7
		10000	7,6	1,2	0,8	0,2	7000000	480000	11,5	3
8	104	100	77	23	15	3,8	14300	3200	16,7	2,9
		1000	76	24	55	12	870000	38000	45	5
		10000	34	27	57	8	8650000	43000	42	7
9	95	100	249	215	18	3	72000	11000	38	11,5
		1000	248	235	21	3,2	630000	42000	36	8
		10000	248	234	24,5	0,5	7120000	1050000	37	12
10	68	100	670	480	1,9	0,5	24500	1800		
		1000	660	510	2,4	0,5	653000	43500	34,5	5,2
		10000	660	512	3	0,25	6250000	254000	34	4,3



460	List of figures
461	
462	Fig.1 Location map of the study area
463	Fig.2 General view of the study area
464	Fig.3 Geological map of the Ermenek region
465	Fig.4 Maps of the study area, and their distributions of (a) altitude, (b) slope gradient,
466	(c) slope aspect
467	Fig.5 Systematic sampling locations along X-X' line
468	Fig.6 Contour diagram of major discontinuity sets
469	Fig.7 Discontinuity spacing histogram
470	Fig.8 Kinematic analysis results of the slopes
471	Fig.9 Fallen blocks and their sizes
472	Fig.10 Rockfall source areas of the Ermenek region
473	Fig.11 Rockfall profiles analyzed in the study area
474	Fig.12 Photograph showing hanging blocks and their location in the study area
475	Fig.13 Back analyses in the field to determine the coefficient of restitutions
476	Fig.14 Distribution of fallen and hanging blocks of the rockfall source areas
477	Fig.15 An example for the rockfall analyses results (a) runout distance (b) total
478	kinetic energy (c) bounce height (d) the typical rockfall trajectory
479	Fig.16 The map showing the rockfall danger zone of study area
480	
481	
482	
483	
484	
485	
486	
487	
488	
489	
490	
491	
492	
493	

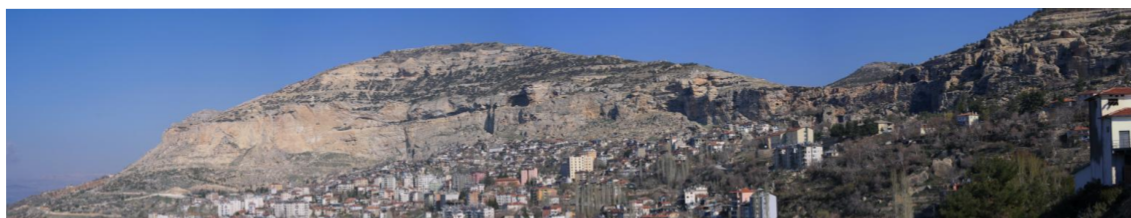


494
495

Fig.1 Location map of the study area

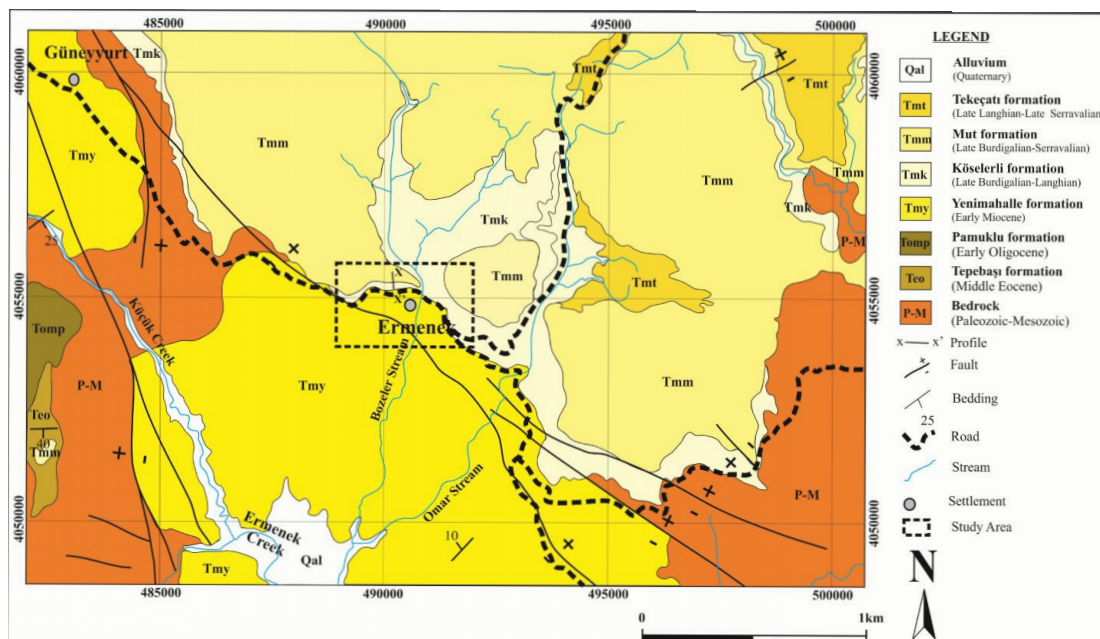


496



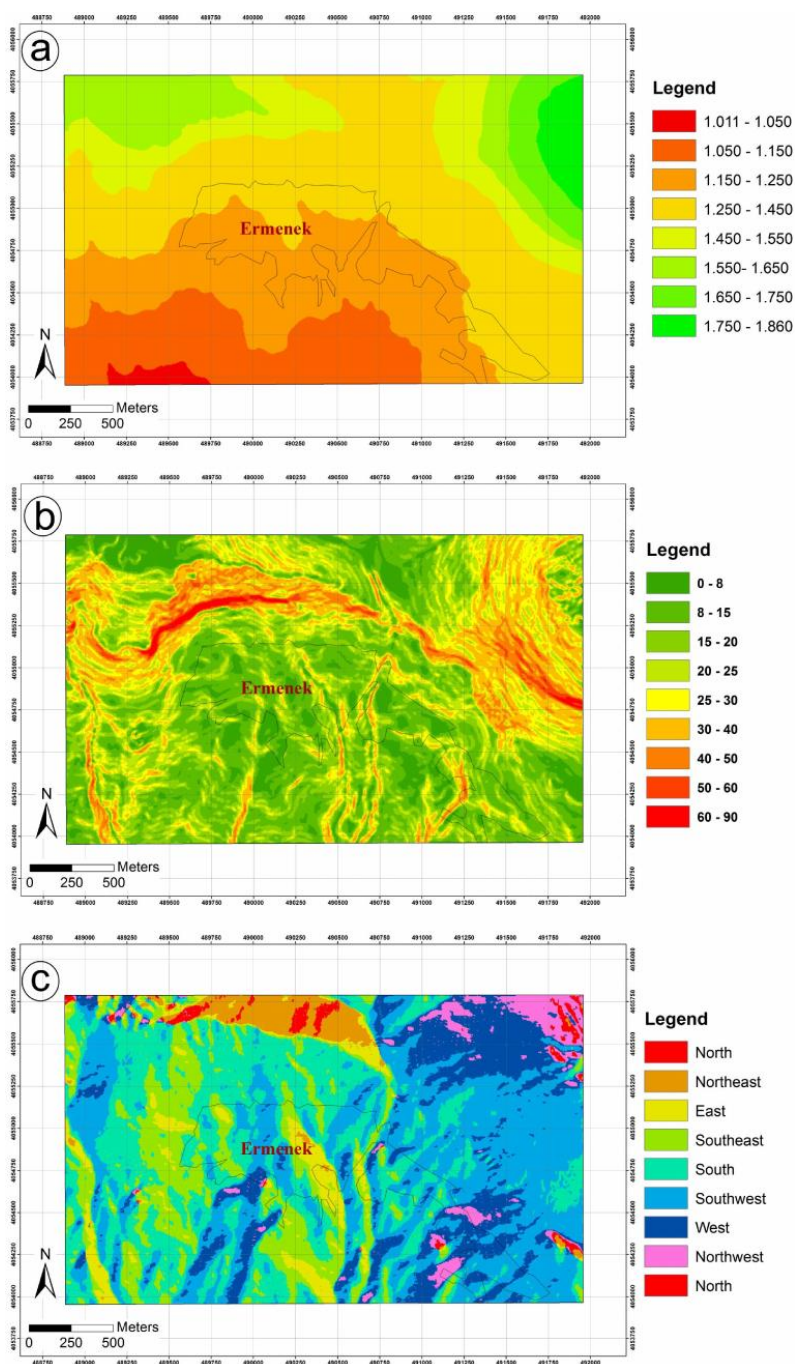
497
498
499
500
501

Fig.2 General view of the study area



502
 503
 504

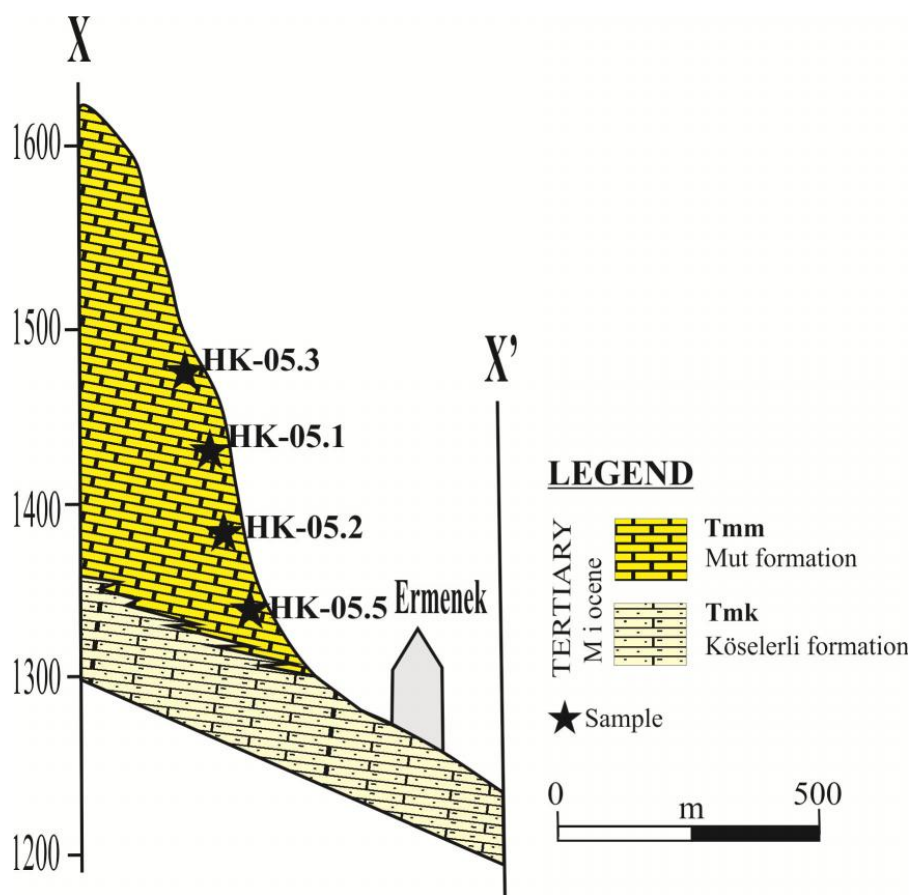
Fig.3 Geological map of the Ermenek region



505

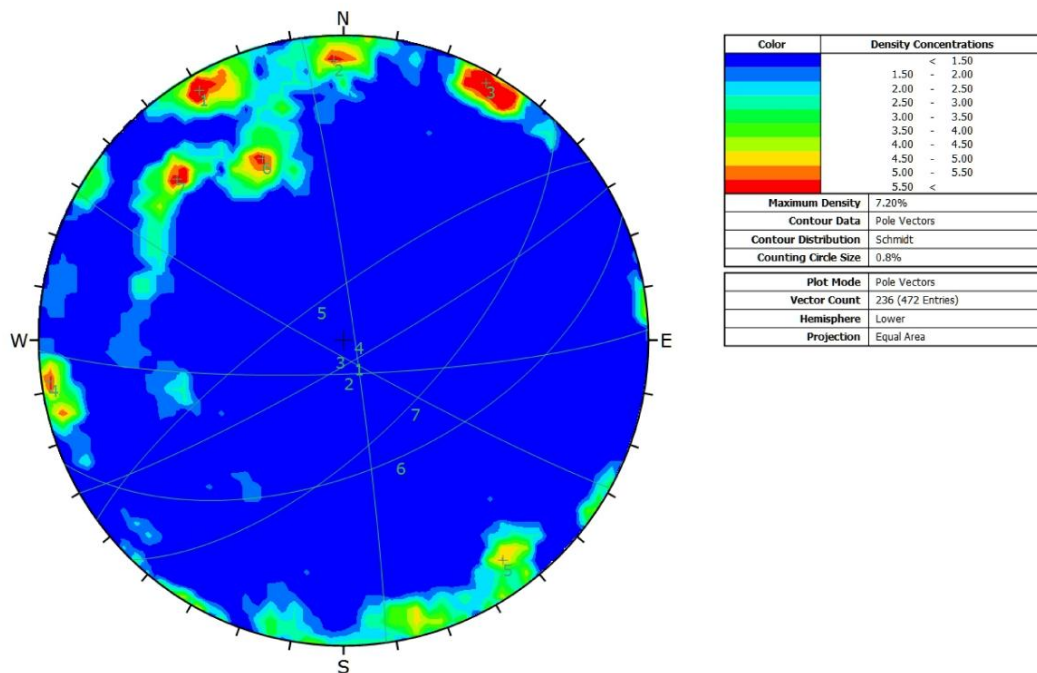
506

507 **Fig.4** Maps of the study area, and their distributions of (a) altitude, (b) slope gradient,
508 (c) slope aspect



509
510
511

Fig.5 Systematic sampling locations along X-X' line

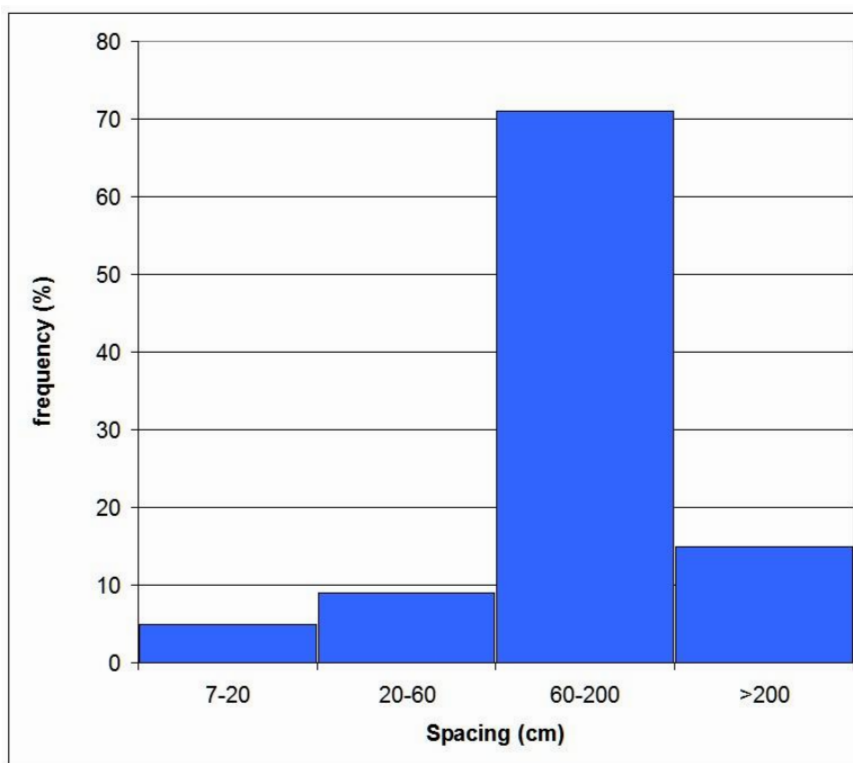


512
 513
 514
 515

Fig.6 Contour diagram of major discontinuity sets



516

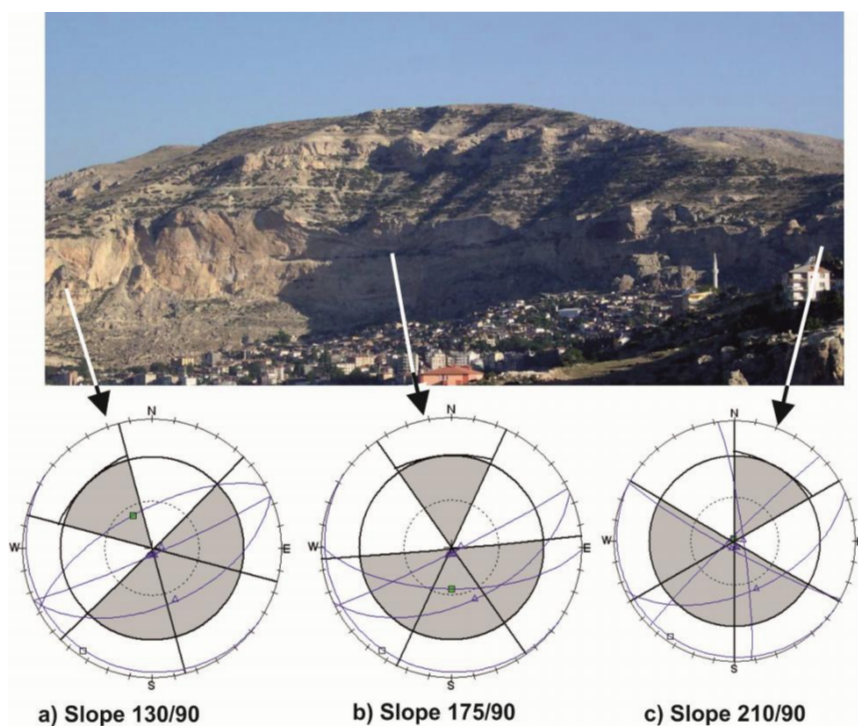


517

518

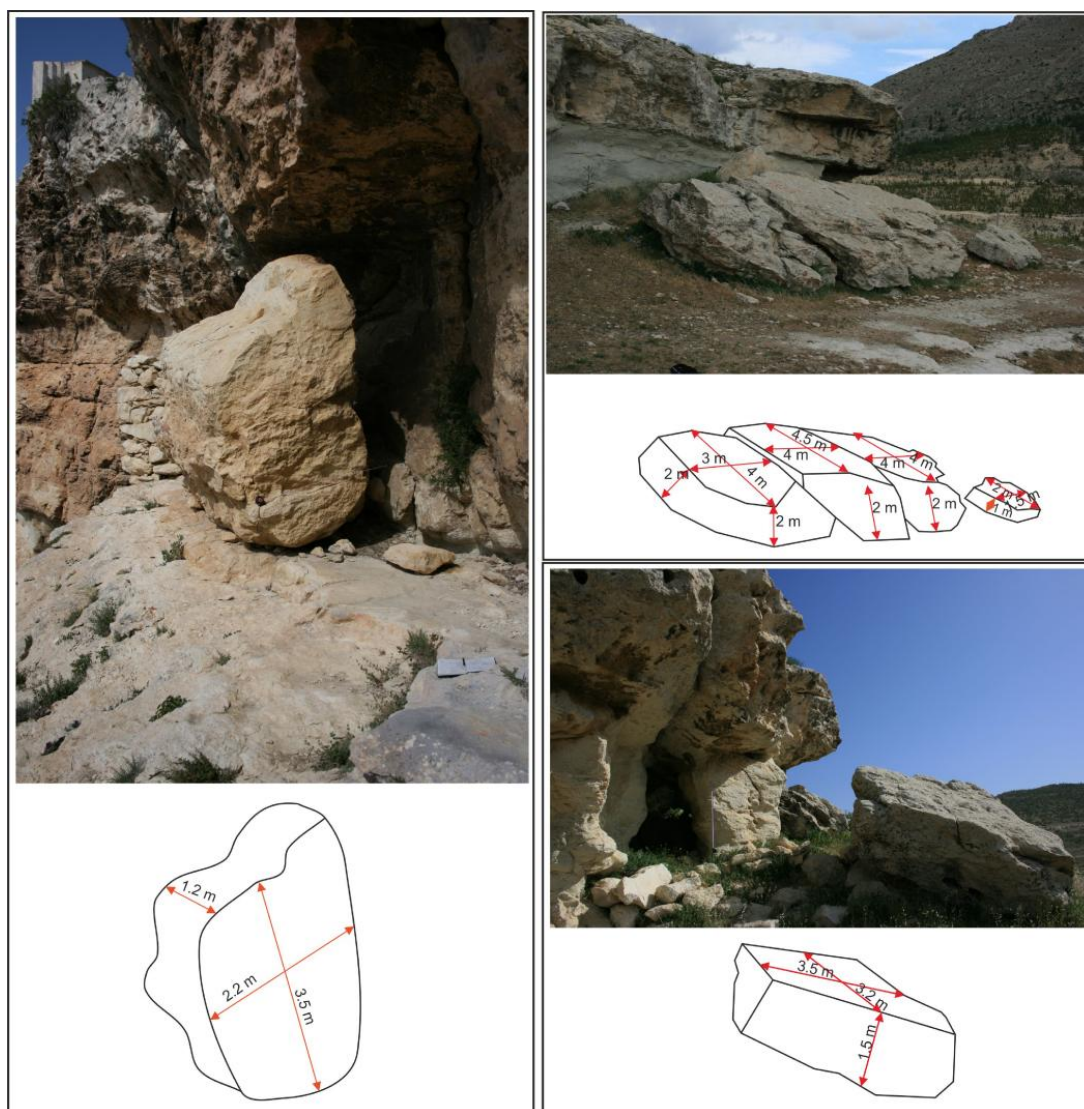
519

Fig.7 Discontinuity spacing histogram



520
521
522

Fig.8 Kinematic analysis results of the slopes

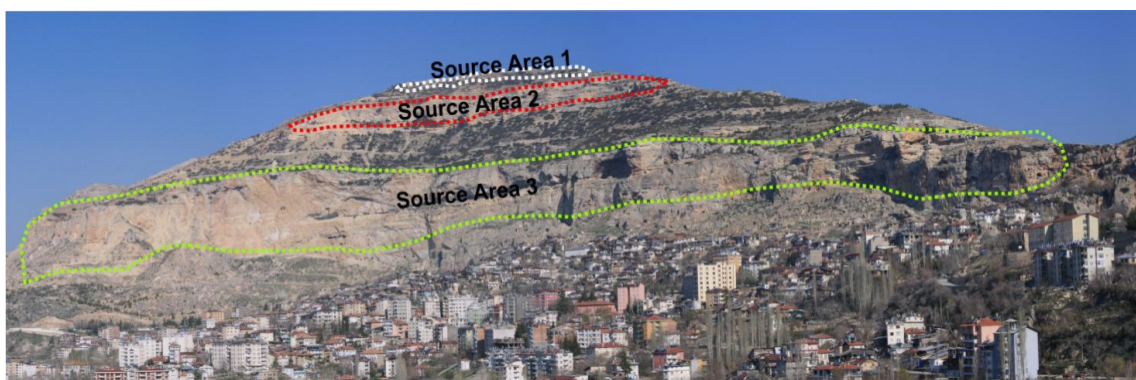


523
524
525

Fig.9 Fallen blocks and their sizes

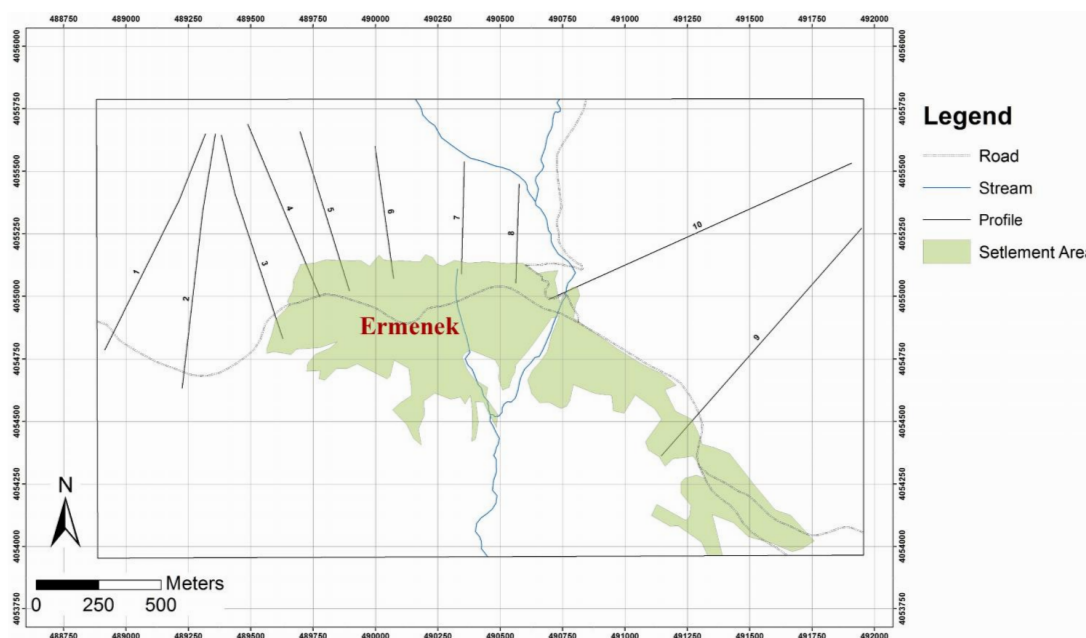


526
527
528
529



530
531
532

Fig.10 Rockfall source areas of the Ermenek region



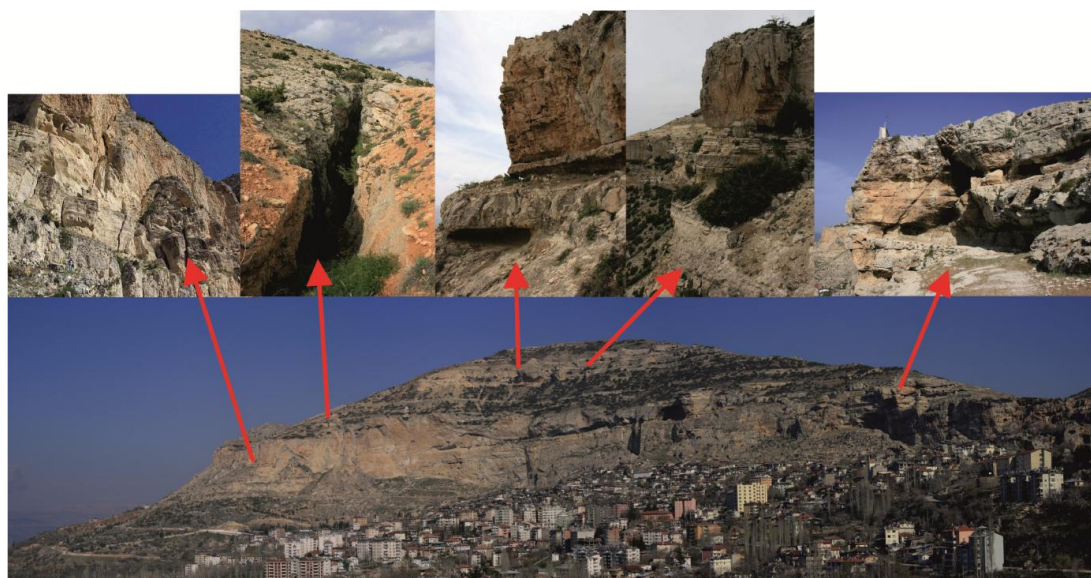
533

534

Fig.11 Rockfall profiles analyzed in the study area



535

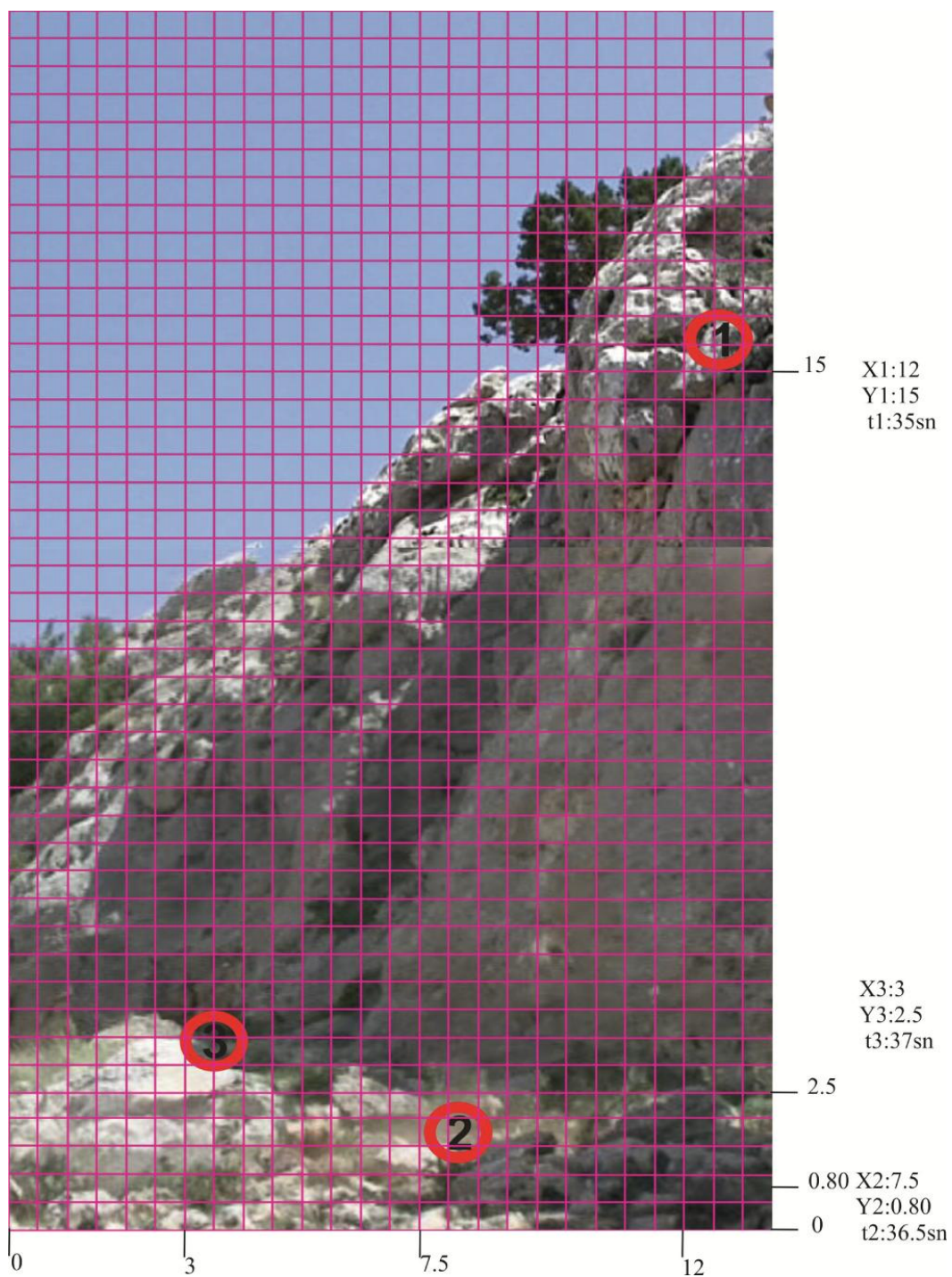


536

537

538

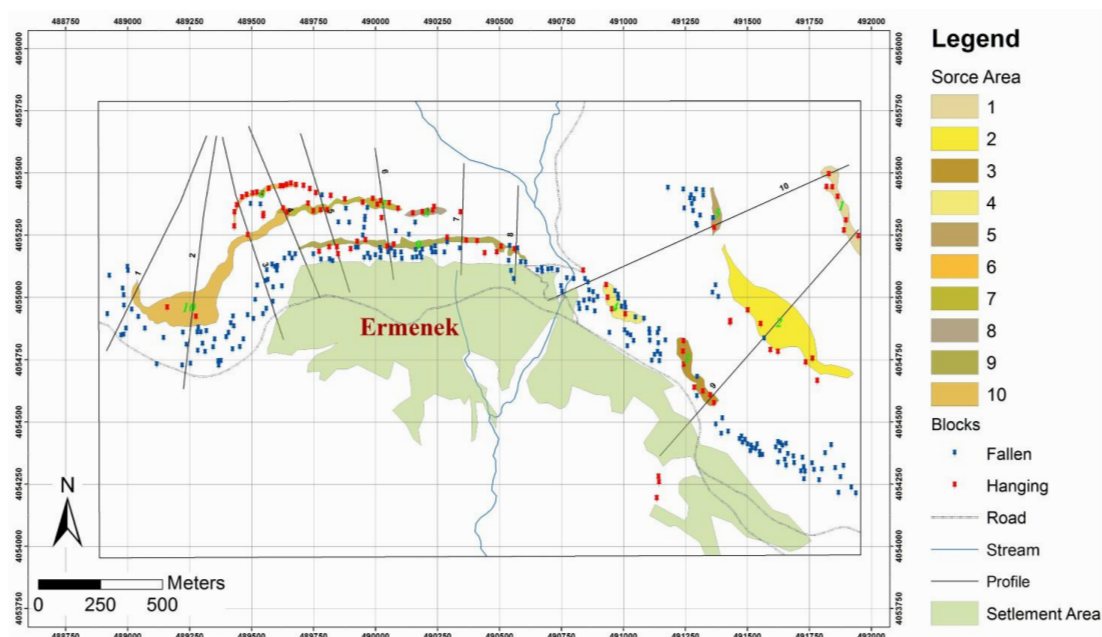
Fig.12 Photograph showing hanging blocks and their location in the study area



539

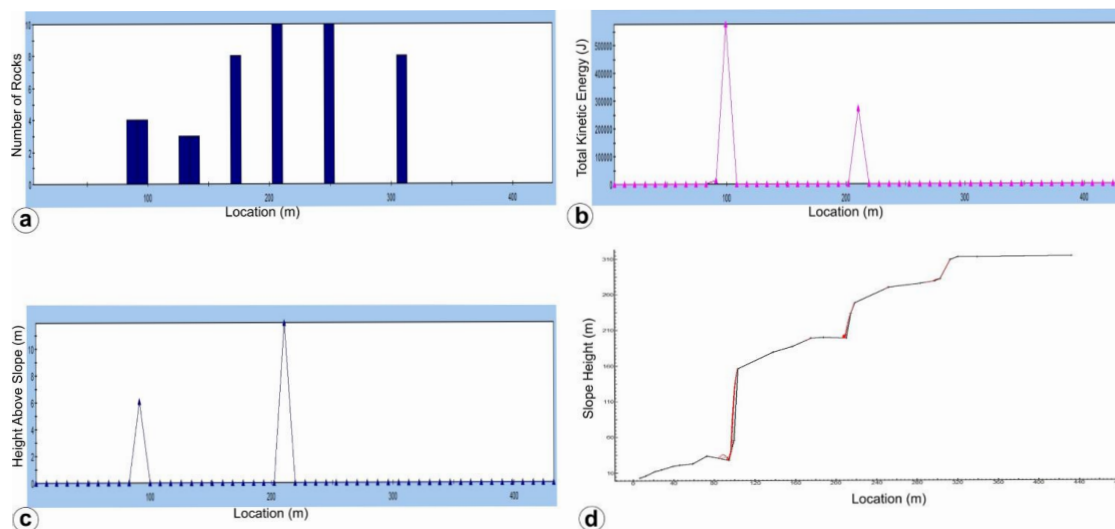
540 **Fig.13** Back analyses in the field to determine the coefficient of restitutions

541

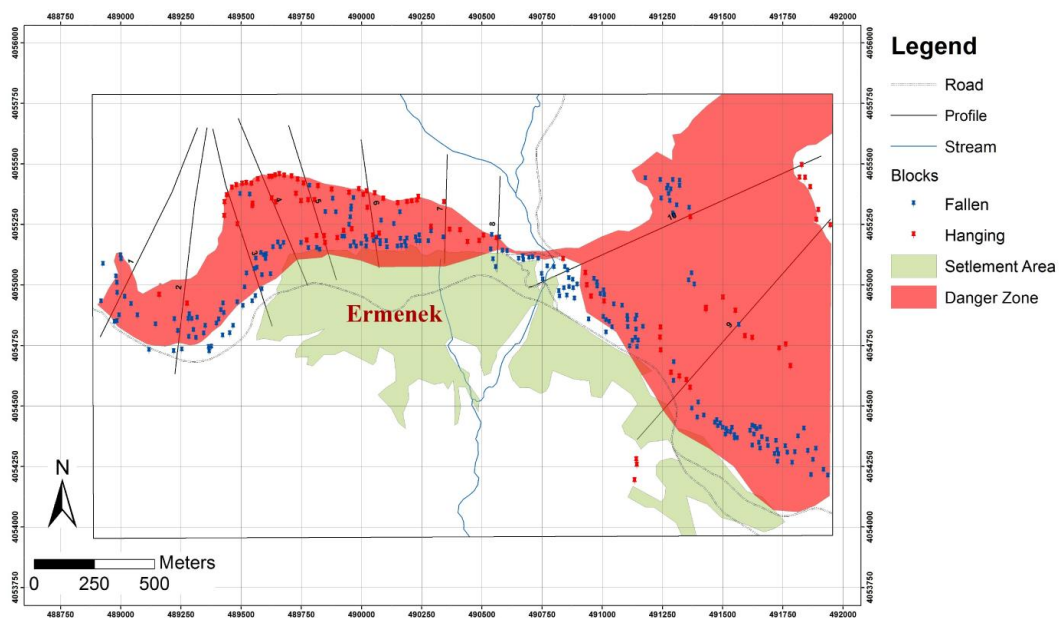


542
543
544

Fig.14 Distribution of fallen and hanging blocks of the rockfall source areas



545
546 **Fig Fig.15** An example for the rockfall analyses results (a) runout distance (b) total kinetic energy (c) bounce height (d) the typical
547 rockfall trajectory



548
549
550

Fig.16 The map showing the rockfall danger zone of study area